Available online at www.sciencedirect.com
ScienceDirect
Ceramics International 37 (2011) 1515–1519
CERAMICS INTERNATIONAL
www.elsevier.com/locate/ceramint

Microwave dielectric properties of the $(1-x)Mg_2TiO_4$–$xCaTiO_3$–y wt.% $ZnNb_2O_6$ ceramics system

Hui Zhu, Wen-Zhong Lu *, Wen Lei

Department of Electronic Science and Technology, Huazhong University of Science and Technology, Wuhan 430074, PR China

Received 7 July 2010; received in revised form 15 November 2010; accepted 7 January 2011
Available online 4 February 2011

Abstract

Composite ceramics based on $(1-x)Mg_2TiO_4$–$xCaTiO_3$–y wt.% $ZnNb_2O_6$ ($x = 0.12$–0.16, $y = 0$–8) were prepared by a conventional mixed-oxide route. Zn^{2+} partially replaced Mg^{2+} in Mg_2TiO_4 and formed the spinel-structured $(Mg_{1-\delta}Zn_\delta)_2TiO_4$ phase. Nb^{2+}, is known to be solid soluble in $CaTiO_3$, was found to change its shape from cubic to pliable. A bi-phase system $(Mg_{1-\delta}Zn_\delta)_2TiO_4$ and $CaTiO_3$ exhibited in all samples, where a small amount of second phase $Mg_{1-\delta}Zn_\delta TiO_3$ was also detected. The microwave dielectric properties of specimens were strongly related to $ZnNb_2O_6$ and $CaTiO_3$ content. As y increased, ε_r and τ_f decreased, however, $Q \times f$ decreased to a minimum value and started to increase thereafter. It was also found that ε_r and τ_f increased and $Q \times f$ decreased with increasing x. The optimized microwave dielectric properties with $\varepsilon_r = 18.37$, $Q \times f = 31{,}027$ GHz (at 6 GHz), and $\tau_f = 0.51$ ppm/°C were achieved for $(1-x)Mg_2TiO_4$–$xCaTiO_3$–y wt.% $ZnNb_2O_6$ ($x = 0.12$, $y = 4$) sintered at 1360 °C for 6 h.

Keywords: Microwave dielectric properties; Mg_2TiO_4; $ZnNb_2O_6$

1. Introduction

With increasing carrier frequency used in communication systems and according to the relation of $\lambda = \lambda_0/\sqrt{\varepsilon_r}$, miniaturization of dielectric resonators becomes less dependent on the dielectric constant. For instance, low loss dielectrics with different dielectric constants have become the most popular materials used for today's GPS patch antennas with different sizes. Requirements of low dielectric constant materials for such high-frequency applications are normally combined with a low dielectric loss ($Q > 5000$, where $Q = 1/\tan\delta$), and a near-zero temperature coefficient of resonant frequency (τ_f) [1]. The most convenient way to achieve a zero τ_f is by combining two materials with a positive and a negative τ_f value to form mixture phases [2].

Spinel titanate ceramic Mg_2TiO_4 ($\varepsilon_r \sim 14$, $Q \times f \sim 150{,}000$ GHz, $\tau_f \sim -50$ ppm/°C) was first reported by Belous [3], followed by more comprehensive researches by Huang [4–8]. $CaTiO_3$ ($\varepsilon_r \sim 170$, $Q \times f \sim 3600$ GHz at 7 GHz, $\tau_f \sim 800$ ppm/°C) [9], significantly improved the dielectric properties of $MgTiO_3$–$CaTiO_3$ system. However, it failed to facilitate the sintering of Mg_2TiO_4–$CaTiO_3$ system [3]. Current methods to improve this system normally use Co to partially substitute Mg [3,5,10] or Sr to partially substitute Ca [6], or even by replacing $CaTiO_3$ with $SrTiO_3$. However, few investigations have been reported on using $ZnNb_2O_6$ to facilitate the sintering of Mg_2TiO_4–$CaTiO_3$ system. In particular, Columbite $ZnNb_2O_6$, with dielectric characteristics of $\varepsilon_r \sim 25$, $Q \times f \sim 83{,}700$ GHz, $\tau_f \sim -56$ ppm/°C at 1150 °C [11], might be a proper material to facilitate sintering as well as to moderate τ_f, and at the same time maintain the low dielectric constant.

Consequently, combining $ZnNb_2O_6$ and Mg_2TiO_4–$CaTiO_3$ not only shows a promotion in sintering, but also achieves an improvement in $Q \times f$ and τ_f compared with that of Mg_2TiO_4–$CaTiO_3$. In addition, the X-ray diffraction (XRD) patterning and scanning electron microscopy (SEM) analysis and an energy-dispersive X-ray spectrometer (EDX) were employed to study the crystal structures and microstructures of the ceramics. The correlation between microwave dielectric properties and $ZnNb_2O_6$ and $CaTiO_3$ content were also investigated.

* Corresponding author. Tel.: +86 27 87542594; fax: +86 27 87543134.
E-mail addresses: hui.zhu2008@gmail.com (H. Zhu), lwz@mail.hust.edu.cn (W.-Z. Lu), navy77@163.com (W. Lei).

0272-8842/$36.00
doi:10.1016/j.ceramint.2011.01.015

2. Experimental procedure

Ceramics based on system $(1-x)Mg_2TiO_4$–$xCaTiO_3$–y wt.% $ZnNb_2O_6$ were produced by the conventional solid-state method. Reagent-grade powders MgO (98.5%), TiO_2 (99.6%), $CaCO_3$ (99.5%), ZnO (99.5%), and Nb_2O_6 (99.99%) were used as starting reagents, and then mixed according to the stoichiometry to form Mg_2TiO_4, $CaTiO_3$ and $ZnNb_2O_6$ powders. After milling in ethanol with zircon balls for 3 h, the mixtures of Mg_2TiO_4, $CaTiO_3$ and $ZnNb_2O_6$ powders were dried and calcined at 1200 °C, 1100 °C and 960 °C, respectively, for 3 h in air. The three calcined powders were subsequently mixed according to the desired stoichiometry. All mixtures were re-milled, dried, screened, added with 5 wt.% of polyvinyl alcohol (PVA), and pressed into pellets with dimensions of 15 mm in diameter and 10 mm in thickness. These pellets were then sintered at 1340–1380 °C for 6 h in air.

The crystalline phases of the sintered ceramics were identified by X-ray diffraction method (XRD) using CuKα radiation (X'Pert PRO). The microstructure observations and quantitative analysis were performed using scanning electron microscope (SEM; FEI-Sirion 200) and an energy-dispersive X-ray spectrometer (EDX, Genesis 7000). The apparent densities of the sintered specimens were measured by the Archimedes method. The dielectric constant (ε_r) and $Q \times f$ were measured using the Hakki–Coleman method [12] with an Advantest R3767C network analyzer and parallel silver boards. An identical technique was applied to the measurement of the temperature coefficient of resonator frequency (τ_f). The test set was placed over a thermostat in the temperature range of 25–80 °C. And τ_f (ppm/°C) was calculated by formula (1):

$$\tau_f = \frac{f_2 - f_1}{f_1(T_2 - T_1)} \quad (1)$$

where f_1 is the resonant frequency at T_1 and f_2 is the resonant frequency at T_2.

3. Results and discussion

3.1. System $0.86Mg_2TiO_4$–$0.14CaTiO_3$–y wt.% $ZnNb_2O_6$

Sintering temperature of Mg_2TiO_4–$CaTiO_3$ ceramics was found to slightly decrease with the incorporation of $ZnNb_2O_6$. The XRD patterns of $0.86Mg_2TiO_4$–$0.14CaTiO_3$–y wt.% $ZnNb_2O_6$ (y = 2, 4, 6, and 8) ceramics sintered at 1360 °C for 6 h (Fig. 1) showed a two-phase system with $(Mg_{1-\delta}Zn_\delta)_2TiO_4$ (indexed as Mg_2TiO_4) and $CaTiO_3$. A second phase $Mg_{1-\delta}Zn_\delta TiO_3$ (indexed as $MgTiO_3$) was observed for $y \leq 4$. The result indicates that $ZnNb_2O_6$ could inhibit the thermal decomposition of $(Mg_{1-\delta}Zn_\delta)_2TiO_4$. With increasing $ZnNb_2O_6$ content, the lattice parameter a of $(Mg_{1-\delta}Zn_\delta)_2TiO_4$ increased to a maximum at y = 4 and decreased thereafter as shown in Fig. 2. This is due to the ionic radii of Zn^{2+} (0.74 Å) being larger than that of Mg^{2+} (0.72 Å). These results agree well with the report by Huang and Liu [13] in which the solid solution limit of Zn in Mg_2TiO_4 was small.

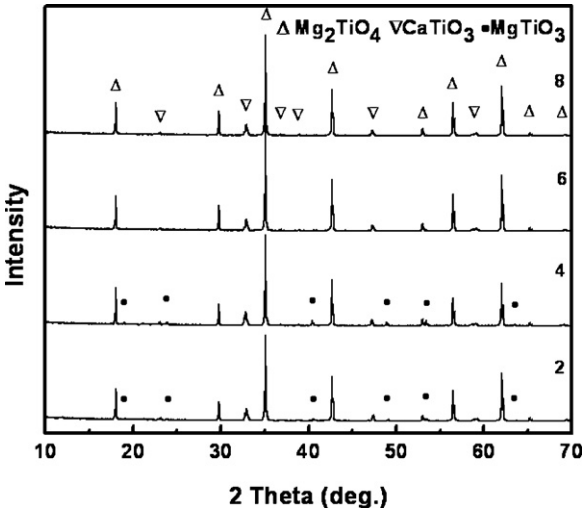

Fig. 1. XRD patterns of $0.86Mg_2TiO_4$–$0.14CaTiO_3$–y wt.% $ZnNb_2O_6$ ceramics sintered at 1360 °C for 6 h.

Fig. 3 shows SEM micrographs of $0.86Mg_2TiO_4$–$0.14CaTiO_3$–y wt.% $ZnNb_2O_6$ (y = 0, 2, 4, and 6) sintered at 1360–1400 °C for 6 h. All samples were well sintered and formed fine-grained structures except for y = 0, and a porous microstructure and an inhomogeneous grain growth was also observed. The porosity decreased with increasing $ZnNb_2O_6$ content. In addition, grain uniformity degraded significantly at y = 4 but recovered thereafter at y = 6 as grain growth (Fig. 3(c) and (d)), which may suggest the trend of quality factor. Moreover, for y = 0, we observed the presence of $MgTi_2O_5$ and found that the ceramic dielectric properties were greatly degraded due to its low $Q \times f$. For $y > 0$, $MgTi_2O_5$ disappeared and $Mg_{1-\delta}Zn_\delta TiO_3$ appeared. $Mg_{1-\delta}Zn_\delta TiO_3$ was not observed in the SEM photographs due to its too little content. Unlike $MgTi_2O_5$, $Mg_{1-\delta}Zn_\delta TiO_3$ had little impact on ceramics dielectric properties, as Su and Wu [14] found that $Mg_{1-\delta}Zn_\delta TiO_3$ and Mg_2TiO_4 had similar microwave dielectric properties.

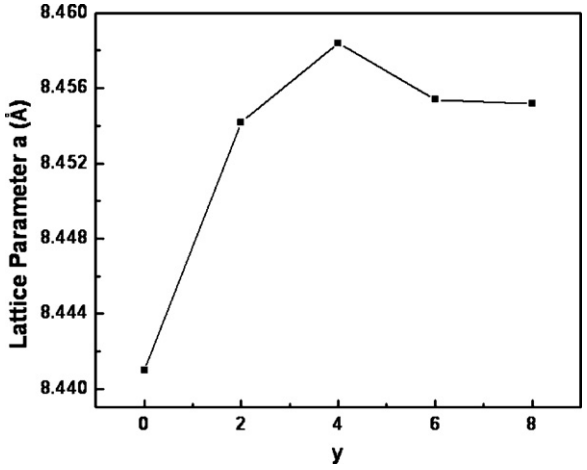

Fig. 2. Lattice parameter a of $0.86Mg_2TiO_4$–$0.14CaTiO_3$–y wt.% $ZnNb_2O_6$ ceramics sintered at 1360 °C for 6 h.

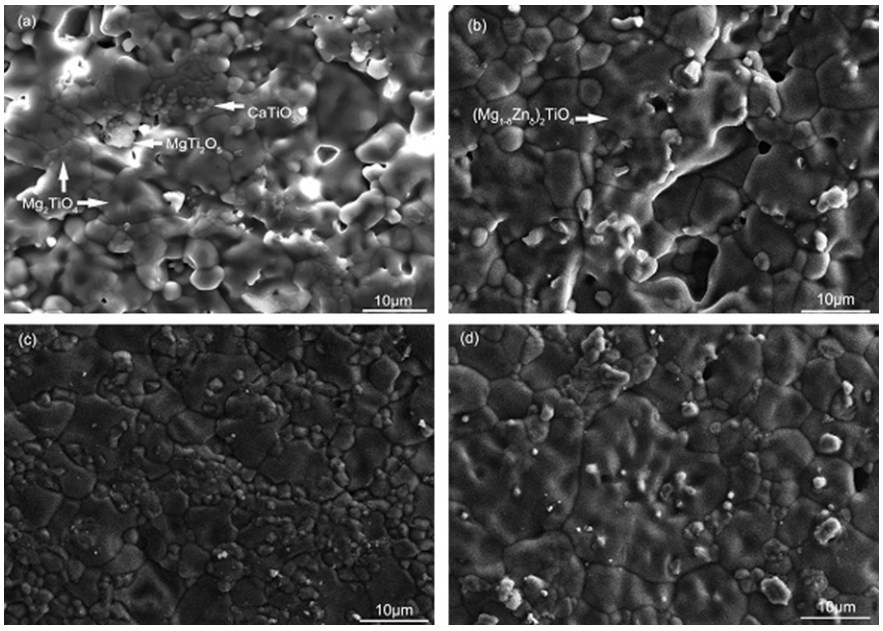

Fig. 3. SEM micrographs of $0.86Mg_2TiO_4$–$0.14CaTiO_3$–y wt.% $ZnNb_2O_6$ ceramics with various y: (a) $y = 0$ sintered at 1400 °C for 6 h; (b), (c), and (d) are $y = 2, 4, 6$, sintered at 1360 °C, respectively.

The apparent densities and the dielectric constant of $0.86Mg_2TiO_4$–$0.14CaTiO_3$–y wt.% $ZnNb_2O_6$ ceramics sintered at temperatures 1340–1380 °C for 6 h are shown in Figs. 4 and 5, respectively. The variation of ε_r was consistent with that of densities, which increased with increasing sintering temperature and decreased with increasing $ZnNb_2O_6$ content when $y > 0$. The reduction of apparent densities and ε_r mainly results from the inhomogeneous grain growth as observed in Fig. 3.

The $Q \times f$ of $0.86Mg_2TiO_4$–$0.14CaTiO_3$–y wt.% $ZnNb_2O_6$ ceramics sintered at 1340–1380 °C for 6 h is plotted in Fig. 6. Since much less pores and no $MgTi_2O_5$ existed, all samples displayed higher $Q \times f$ than $0.86Mg_2TiO_4$–$0.14CaTiO_3$ ceramics did ($Q \times f \sim 23{,}297$ GHz for $0.86Mg_2TiO_4$–$0.14CaTiO_3$ ceramics). Moreover, $Q \times f$ decreased slightly when y increased to 4, and increased thereafter with increasing y. The decrease in $Q \times f$ could be attributed to the increase in inhomogeneous grain growth, as shown in Fig. 3 that

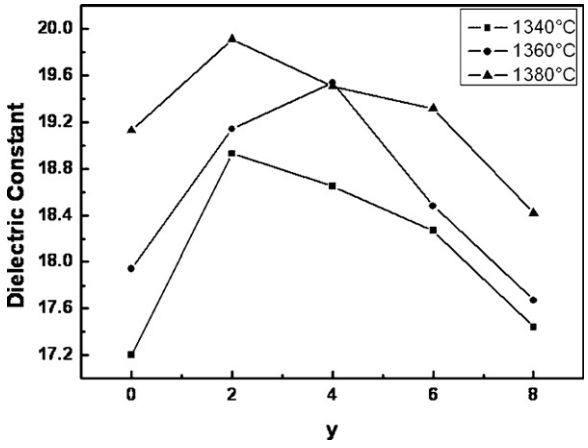

Fig. 5. Dielectric constant of $0.86Mg_2TiO_4$–$0.14CaTiO_3$–y wt.% $ZnNb_2O_6$ ceramics sintered at 1340–1380 °C for 6 h.

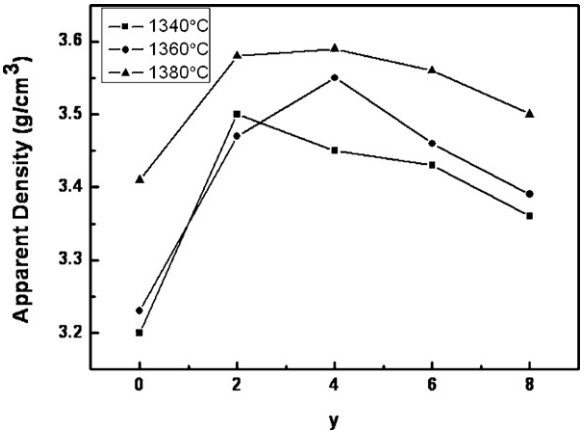

Fig. 4. Apparent densities of $0.86Mg_2TiO_4$–$0.14CaTiO_3$–y wt.% $ZnNb_2O_6$ ceramics sintered at 1340–1380 °C for 6 h.

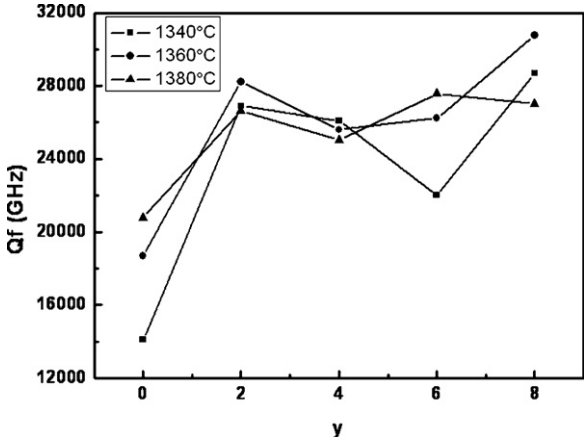

Fig. 6. $Q \times f$ of $0.86Mg_2TiO_4$–$0.14CaTiO_3$–y wt.% $ZnNb_2O_6$ ceramics sintered at 1340–1380 °C for 6 h.

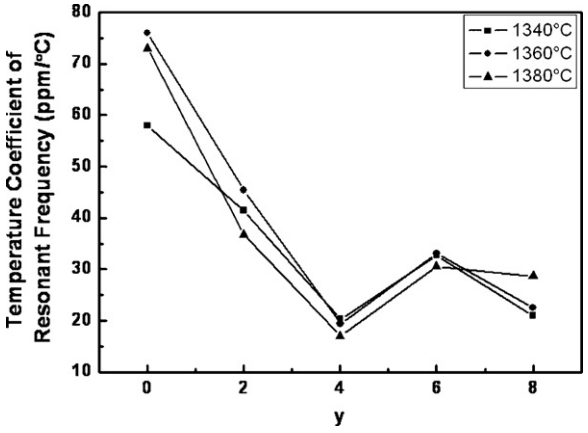

Fig. 7. τ_f of $0.86Mg_2TiO_4$–$0.14CaTiO_3$–y wt.% $ZnNb_2O_6$ ceramics sintered at 1340–1380 °C for 6 h.

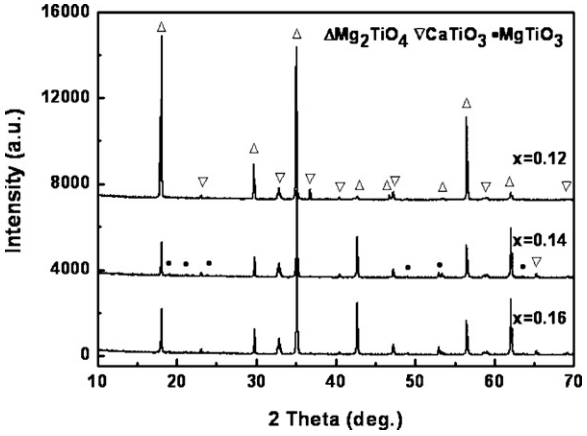

Fig. 8. XRD patterns of $(1-x)Mg_2TiO_4$–$xCaTiO_3$–4 wt.% $ZnNb_2O_6$ ceramics sintered at 1360 °C for 6 h.

inhomogeneous grain growth appeared to be the worst at $y = 4$, leading to an increase in lattice imperfection and dielectric loss. The increase in $Q \times f$ showed a different trend from that of apparent density. It could be a result of fewer pores and grain boundaries. However, the inhomogeneous grain growth is still the main reason for low $Q \times f$.

Fig. 7 shows τ_f of $0.86Mg_2TiO_4$–$0.14CaTiO_3$–y wt.% $ZnNb_2O_6$ ceramics sintered at 1340–1380 °C for 6 h. The τ_f is well known to be governed by composition, additives and second phase of the materials. Increasing $ZnNb_2O_6$ content seemed to make τ_f more negative, since the τ_f of $ZnNb_2O_6$ is −56 ppm/°C. In addition, a significant change appeared at $y = 6$, showing a dependence on the second phase $Mg_{1-\delta}Zn_\delta TiO_3$ in the specimens.

We expected that $Q \times f$ could still keep high and τ_f could be lowered to near 0 ppm/°C, so we changed the content of $CaTiO_3$ and $ZnNb_2O_6$ based on a mixing rule for composite materials and the implication that we found from our research. After a series of experiments, we fixed at 4 wt.% $ZnNb_2O_6$ in the following discussion to observe the function of $CaTiO_3$ in the system.

3.2. System $(1-x)Mg_2TiO_4$–$xCaTiO_3$–4 wt.% $ZnNb_2O_6$

Fig. 8 shows the XRD patterns of $(1-x)Mg_2TiO_4$–$xCaTiO_3$–4 wt.% $ZnNb_2O_6$ ($x = 0.12$, 0.14, 0.16) ceramics sintered at 1360 °C for 6 h. As $CaTiO_3$ content decreased to 12%, the second phase $MgTiO_3$ disappeared, indicating that

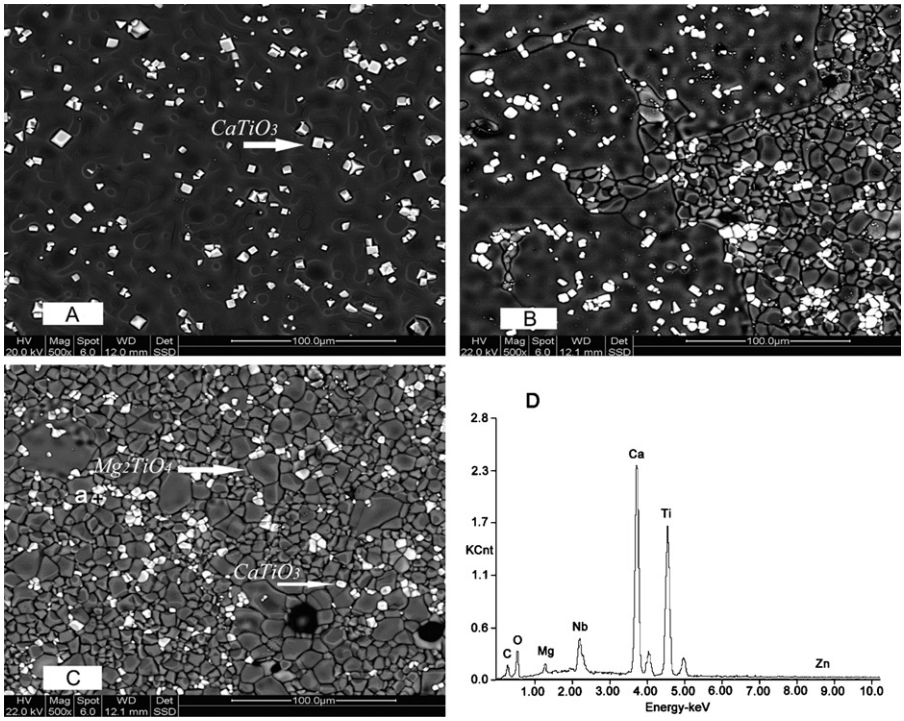

Fig. 9. (A–C) SEM micrographs of natural surfaces of $(1-x)Mg_2TiO_4$–$xCaTiO_3$–4 wt.% $ZnNb_2O_6$ ceramics sintered at 1360 °C for 6 h, and (A), (B), and (C) are $x = 0.12$, 0.14, and 0.16, respectively; (D) EDX for spot a in picture (C).

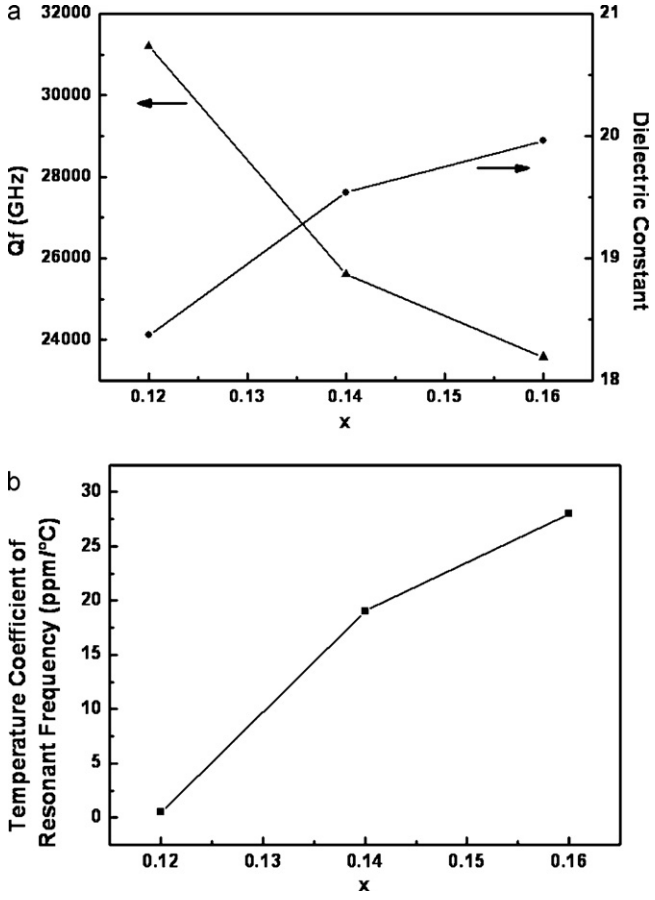

Fig. 10. Microwave dielectric properties of $(1-x)Mg_2TiO_4$–$xCaTiO_3$–4 wt.% $ZnNb_2O_6$ ceramics sintered at 1360 °C for 6 h: (a) $Q \times f$ and ε_r; (b) τ_f.

less $CaTiO_3$ can inhibit the decomposition of Mg_2TiO_4. Meanwhile, the X-ray diffraction intensities of Mg_2TiO_4 significantly enhanced, indicating Mg_2TiO_4 grains grew quickly. This is also supported later by SEM micrographs.

The SEM micrographs of natural surfaces of $(1-x)Mg_2TiO_4$–$xCaTiO_3$–4 wt.% $ZnNb_2O_6$ ceramics sintered at 1360 °C for 6 h are shown in Fig. 9, and (A), (B), and (C) are $x = 0.12$, 0.14, 0.16, respectively. We observed a significant change where Mg_2TiO_4 in the surface rapidly solid-melted together as $CaTiO_3$ content reduced. Moreover, the grain shape of $CaTiO_3$ gradually changed from cubic to a pliable shape as $ZnNb_2O_6$ content increased. This is due to the solid solution of Nb in the perovskite $CaTiO_3$, causing the perovskite lattice to distort. It was confirmed by the EDX (Fig. 9(D)) for spot a in Fig. 9(C). However, the effect of Nb in $CaTiO_3$ needs further investigation.

Fig. 10 shows the microwave dielectric properties of $(1-x)Mg_2TiO_4$–$xCaTiO_3$–4 wt.% $ZnNb_2O_6$ ($x = 0.12$, 0.14, 0.16) ceramics sintered at 1360 °C for 6 h. The correlation between the $CaTiO_3$ content and the system's dielectric properties is very clear. With $CaTiO_3$ content increased form 12% to 16%, τ_f increased from +0.51 ppm/°C to +29.74 ppm/°C, ε_r increased from 18.37 to 19.96, and $Q \times f$ decreased from 31,207 GHz to 24,652 GHz. This is reasonable since the τ_f value of $CaTiO_3$ is +800 ppm/°C, the dielectric constants of Mg_2TiO_4 and $CaTiO_3$ are 14 and 170, respectively, and $CaTiO_3$ has a much lower $Q \times f$ than that of Mg_2TiO_4.

An excellent combination of microwave dielectric characteristics was achieved in the composition of $x = 0.12$, $y = 4$, with $\varepsilon_r = 18.37$, $Q \times f = 31{,}027$ GHz (at 6 GHz), and $\tau_f = 0.51$ ppm/°C.

4. Conclusions

In this paper, the effect of different $ZnNb_2O_6$ and $CaTiO_3$ compositions in xMg_2TiO_4–$(1-x)CaTiO_3$–y wt.% $ZnNb_2O_6$ ceramics were investigated. The microwave dielectric properties are strongly related to the matrix of the specimen. At the composition of $x = 0.12$, $y = 4$, the ceramics sintered at 1360 °C/6 h, have excellent microwave dielectric properties: $\varepsilon_r = 18.37$, $Q \times f = 31{,}027$ GHz, and $\tau_f = 0.51$ ppm/°C. Our results strongly suggest that Mg_2TiO_4–$CaTiO_3$–y wt.% $ZnNb_2O_6$ ceramics are promising for GPS patch antenna application.

Acknowledgements

This work is supported by Program for New Century Excellent Talents in University (NCET-07-0329). The authors are grateful to Analytical and Testing Center, Huazhong University of Science and Technology for XRD and SEM analysis.

References

[1] C.L. Huang, C.H. Shen, C.L. Pan, Materials Science and Engineering B: Solid State Materials for Advanced Technology 145 (1–3) (2007) 91–96.
[2] M.T. Sebastian, Dielectric Materials for Wireless Communication, Elsevier, Amsterdam, 2008, pp. 513–523.
[3] A. Belous, Journal of the American Ceramic Society 89 (11) (2006) 3441–3445.
[4] C.-L. Huang, J.-Y. Chen, C.-Y. Jiang, Journal of Alloys and Compounds 487 (1–2) (2009) 420.
[5] C.L. Huang, J.Y. Chen, Journal of the American Ceramic Society 92 (2) (2009) 379–383.
[6] C.-L. Huang, J.-Y. Chen, Journal of Alloys and Compounds 485 (1–2) (2009) 706–710.
[7] C.-L. Huang, S.S. Liu, Journal of Alloys and Compounds 471 (1–2) (2009) L9–L12.
[8] C.-L. Huang, S.S. Liu, S.H. Chen, Journal of Alloys and Compounds 480 (2) (2009) 794.
[9] R.C. Kell, A.C. Greenham, G.C.E. Olds, Journal of the American Ceramic Society 56 (7) (1973) 352–354.
[10] A. Belous, Journal of the European Ceramic Society 27 (8–9) (2007) 2963–2966.
[11] M. Maeda, T. Yamamura, T. Ikeda, Japanese Journal of Applied Physics, Supplement 26 (1987) 76–79.
[12] B.W. Hakki, P.D. Coleman, Transactions on IRE 8 (4) (1960) 402–410.
[13] C.-L. Huang, S.S. Liu, Journal of the American Ceramic Society 91 (10) (2008) 3428–3430.
[14] H. Su, S.H. Wu, Materials Letters 59 (18) (2005) 2337–2341.